

impact craters in all the images shown here is obvious. A number of small impact craters can be seen on top of some of the translated and rotated blocks in Fig. 3, but the low-lying material between the blocks is practically devoid of craters. From the latest estimate of the comet impact flux on Europa²³, and assuming plausible ratios of smaller comets to the observable larger ones²⁴, and that the observed craters are primaries, not secondaries, the age of the fractured surface is estimated to be of the order of 10⁷ yr. With the same assumptions, the intervening materials are younger, perhaps a few million years old. Parts of the disrupted zone are overlain by rays from Pwyll crater and some of the craters appear to be Pwyll secondaries, not primaries. If this were taken into account, the derived ages would be even younger. As the uniquely prominent ray system of Pwyll suggests, it is the most recent large crater to have formed on Europa. Such craters are expected to form about every 10⁶ yr. According to this model, even with the uncertainties in the cratering rates²³, it is difficult to see how the inter-block material, appearing so sparsely cratered at a resolution of 54 m per pixel, could be much older than 10⁸ yr. (However, a minority of the authors of this Letter hold that the age of the surface can be better estimated by assuming that the youngest basin of Ganymede is 3.8 × 10⁹ yr old, then deriving subsequent cratering rates from the number of craters superimposed on the basin and assuming a lunar decay constant for the cratering rate. This method yields a date of ~3 × 10⁹ yr for the area discussed here; G.N., manuscript in preparation). Although we cannot assert unequivocally that water is present today below the region shown in Fig. 1, if the young age of 10⁸ yr—only a few per cent of the age of Europa—is correct, then the processes that have disrupted the plains are almost certainly continuing today, and liquid water is widely present at depths that are shallow compared with the 150-km estimated thickness of the water/ice layer. □

Received 19 May; accepted 5 November 1997.

1. Kuiper, G. P. *Planets and Satellites* (Univ. Chicago Press, 1961).
2. Moroz, V. I. Infrared spectrophotometry of the Moon and the Galilean satellites of Jupiter. *Astron. A. J.* **9**, 999–1006.
3. Morrison, D. & Cruikshank, D. P. Physical properties of the natural satellites. *Space Sci. Rev.* **15**, 641–739 (1974).
4. Anderson, J. D., Lau, E. L., Sjogren, W. L., Schubert, G. & Moore, W. B. Europa's differentiated internal structure: Inferences from two Galileo encounters. *Science* **276**, 1236–1239 (1997).
5. Smith, B. A. *et al.* The Galilean satellites and Jupiter: Voyager 2 imaging science results. *Science* **206**, 927–950 (1979).
6. Cassen, P., Reynolds, R. T. & Peale, S. J. Is there liquid water on Europa? *Geophys. Res. Lett.* **6**, 731–734 (1979).
7. Cassen, P., Reynolds, R. T. & Peale, S. J. Tidal dissipation on Europa: A correction. *Geophys. Res. Lett.* **7**, 987–989 (1980).
8. Sqyres, S. W., Reynolds, R. T., Cassen, P. & Peale, S. J. Liquid water and active resurfacing on Europa. *Nature* **301**, 225–226 (1983).
9. Ross, M. & Schubert, G. Tidal heating in an internal ocean model of Europa. *Nature* **325**, 13–14 (1986).
10. Ojakangas, G. W. & Stevenson, D. J. Thermal state of an ice shell on Europa. *Icarus* **81**, 220–241 (1989).
11. Greenberg, R. & Wiedenschilling, S. J. How fast do Galilean satellites spin? *Icarus* **58**, 186–196 (1984).
12. Helfenstein, P. & Parmentier, E. M. Patterns of fractures and tidal stresses due to non-synchronous rotation: Implications for Europa. *Icarus* **612**, 175–184 (1985).
13. McEwen, A. S. Tidal reorientation and the fracturing of Jupiter's moon Europa. *Nature* **321**, 49–51 (1986).
14. Pappalardo, R. T., Head, J. W., Greeley, R. & the Galileo Imaging Team. A Europa ocean? The (circumstantial) geological evidence. in *Proc. Europa Ocean Conf.* 59–60 (1996).
15. Lucchitta, B. L. & Soderblom, L. A. in *Satellites of Jupiter* (ed. Morrison, D.) 521–555 (Univ. Arizona Press, Tucson, 1982).
16. Pappalardo, R. T. & Coon, M. D. A sea analog for the surface of Europa. *Lunar Planet. Sci. Conf.* **XXVII**, 997–998 (1996).
17. Greeley, R. *et al.* Europa: Initial Galileo geological observations. (submitted).
18. Pappalardo, R. T. *et al.* Geological evidence for solid-state convection in Europa's ice shell. *Nature* **391**, 365–368 (1998).
19. Schenk, P. M. & McKinnon, W. B. Fault offsets and lateral crustal movement on Europa: Evidence for a mobile ice shell. *Icarus* **79**, 75–100 (1989).
20. Pappalardo, R. T. & Sullivan, R. J. Evidence for separation across a gray band on Europa. *Icarus* **123**, 557–567 (1996).
21. Sullivan, R. & the Galileo Imaging Team. Galileo views of crustal disruption on Europa. *Lunar Planet. Sci. Conf.* **XXVIII**, 1395–1396 (1997).
22. Tufts, R. B., Greenberg, R., Sullivan, R., Pappalardo, R. & the Galileo Imaging Team. *Lunar Planet. Sci. Conf.* **XXVIII**, 1455–1456 (1997).
23. Shoemaker, E. M. The age of Europa's surface. in *Proc. Europa Ocean Conf.* 65–66 (1996).
24. Chapman, C. R. & the Galileo Imaging Team. Populations of small craters on Europa, Ganymede and Callisto: Initial Galileo imaging results. *Lunar Planet. Sci. Conf.* **XXVIII**, 217–218 (1997).

Correspondence and requests for materials should be addressed to M.H.C. (e-mail: carr@astmnl.wr.usgs.gov).

Geological evidence for solid-state convection in Europa's ice shell

R. T. Pappalardo*, J. W. Head*, R. Greeley†, R. J. Sullivan†, C. Pilcher‡, G. Schubert§, W. B. Moore§, M. H. Carr||, J. M. Moore¶, M. J. S. Belton# & D. L. Goldsby*

* Department of Geological Sciences, Brown University, Providence, Rhode Island 02912-1846, USA

† Department of Geology, Arizona State University, Tempe, Arizona 85287-1404, USA

‡ National Aeronautics and Space Administration Headquarters, 300 East Street SW, Washington DC 20546, USA

§ Department of Earth and Space Sciences, Institute of Geophysics and Planetary Physics, University of California Los Angeles, California 90095-1567, USA

|| United States Geological Survey, 345 Middlefield Road, Menlo Park, California 94025, USA

¶ National Aeronautics and Space Administration, Ames Research Center, Moffett Field, California 94035, USA

National Optical Astronomy Observatories, Tucson, Arizona 85726-6732, USA

The ice-rich surface of the jovian satellite Europa is sparsely cratered, suggesting that this moon might be geologically active today¹. Moreover, models of the satellite's interior indicate that tidal interactions with Jupiter might produce enough heat to maintain a subsurface liquid water layer^{2–5}. But the mechanisms of interior heat loss and resurfacing are currently unclear, as is the question of whether Europa has (or had at one time) a liquid water ocean^{6,7}. Here we report on the morphology and geological interpretation of distinct surface features—pits, domes and spots—discovered in high-resolution images of Europa obtained by the Galileo spacecraft. The features are interpreted as the surface manifestation of diapirs, relatively warm localized ice masses that have risen buoyantly through the subsurface. We find that the formation of the features can be explained by thermally induced solid-state convection within an ice shell, possibly overlying a liquid water layer. Our results are consistent with the possibility that Europa has a liquid water ocean beneath a surface layer of ice, but further tests and observations are needed to demonstrate this conclusively.

During its sixth orbit through the jovian system the Galileo spacecraft obtained high-resolution images (~70 and 180 m per pixel) covering a ~10⁵ km² region of Europa centred near latitude 15° N, longitude 270° W. These images reveal that the satellite's late-stage geology is dominated by circular to elliptical pits, domes and dark spots ~7–15 km in diameter, spaced 5–20 km apart. These features generally modify and disrupt the pre-existing plains, which are widespread and are composed of subparallel ridges and grooves that overlap in successive generations¹. Lower-resolution images show that these features appear to constitute terrain like that of the previously defined “mottled plains” unit of Europa, which occurs over a large portion of the satellite's imaged surface⁶. Therefore, we infer that these pits, domes and spots are probably widespread across Europa, and are suspected to exist where mottled plains units occur.

In the region imaged at high resolution, a range of circular to elliptical features is observed with diverse specific morphologies (Fig. 1). The similarity in size and spacing of pits, domes and spots, and the gradation in morphology among them, suggests that they are genetically related. The features all have altered the original topography through positive or negative vertical deformation, and the vast majority are characterized by a surface morphology which is disrupted. The least-altered structures are characterized by a topo-

graphic rise with no disruption of background structure; somewhat more altered features include median fractures (Fig. 1a, b). The most disrupted features are characterized by a fragmented 'micro-chaos' region on top of the topographic highs, annular depressions, associated smooth low-albedo plains, and chaotic depressions which commonly destroy or embay the pre-existing background structural elements (Fig. 1c–f). Taken together, the structures appear to represent a sequence in which the surface was flexed upwards by intrusion beneath a relatively thin rigid surface layer, and experienced varying degrees of localized heating, collapse and extrusion.

This sequence is consistent with intrusion either by molten material, as would define a laccolithic intrusion, or by warm but relatively viscous solid-state material which rose buoyantly, through diapiric intrusion. We favour a diapiric origin of pits, domes and spots over laccolithic emplacement related to dyke intrusion, on the basis of the widespread occurrence, apparent spatial randomness relative to pre-existing structures, and general uniformity in diameter and spacing of these features. Based on the characteristics outlined in Fig. 1a–f, we propose a model in which diapirs of warm ice have risen from the deeper subsurface and have penetrated to within a few kilometres of the surface (Fig. 1g), that is, to a depth equivalent to about half the diameter of the zone of the most intense mechanical and thermal deformation. In some cases, rising diapirs are interpreted to have altered the surface topography and morphology by creating only a broad rise (Fig. 1g, left). In many cases, rising diapirs are interpreted to have affected more severely the surface and near surface (Fig. 1g, right), causing extension, deformation and possible sublimation and localized melting of the overlying surface, to produce 'micro-chaotic' terrain. The observed smooth, relatively low-albedo material (Fig. 1f) suggests thermal alteration of the surface⁸ or localized extrusion of melt, perhaps

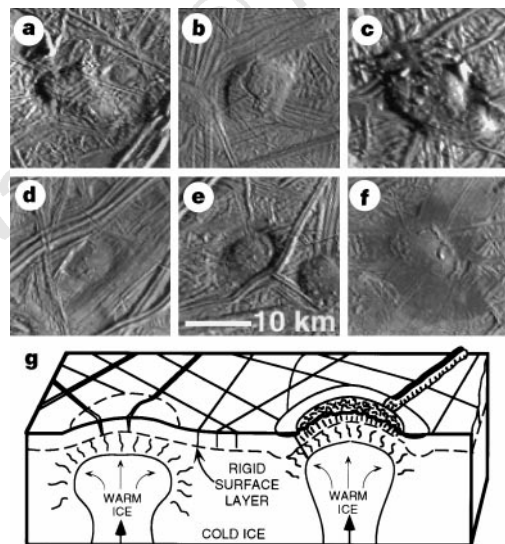


Figure 1 Pits, domes and spots of various specific morphologies (shown to a common scale) on the surface of Europa. North is to the top and illumination is from the east. **a**, A dome which has flexed upwards pre-existing plains material without disrupting it; **b**, a dome with a median fracture; **c**, a disrupted plateau, suggesting a combination of uplift and disruption of material; **d**, a depression with disrupted 'micro-chaos' material; **e**, a disrupted plateau with a depressed annulus; and **f**, a disrupted area with an annulus of dark smooth material. **g**, Block diagram illustrating the interpretation of these features as due to diapiric rise of warm ice, and mechanical and thermal alteration of the surface and near surface.

produced locally if a warm ice diapir contacts a pocket of low-melting-point brine or ice⁹. The marginal moat commonly associated with pits and spots is possibly a "rim syncline"¹⁰ formed by downward flexing of the surface above the region from which rising diapiric material is withdrawn.

Diapirism can be triggered by compositional layering, producing density inversions and gravitational instabilities, as in regional salt layers underlying denser rocks on Earth¹¹ and as suggested for pits on Triton¹². Diapirism also can be induced thermally by means of solid-state convection, which may occur within any icy body if a sufficient thermal gradient exists, especially if the temperature at the base of the ice layer is near the solidus¹³. Models for the internal structure of Europa suggest that tidal heating might be sufficient to maintain a liquid water ocean ~10–30 km beneath its surface, its modelled depth varying with latitude and longitude^{2–5}. Reynolds and Cassen¹⁴ have investigated a model in which a liquid water layer might drive solid-state convection within a large icy satellite, such as Europa. Here we re-evaluate this solid-state convection model, using recently updated parameters describing the flow of ice in which strain rate is a function of stress, temperature and ice grain size^{15,16}.

Convection in an icy satellite would be expected to occur in a warmer sublayer beneath a cold brittle surface lid. The critical Rayleigh number Ra describing the onset of convection is related to the thickness *h* of the sublayer and the temperature difference Δ*T* across it as:

$$Ra = \rho g h^3 \alpha \Delta T / (\kappa \eta). \quad (1)$$

Here ρ is density, α is thermal expansivity, κ is thermal diffusivity and η is viscosity. We choose $Ra \approx 2,000$ as appropriate to a variable-viscosity fluid¹⁷ and consider the range 500–3,500 to cover uncertainty in this value. Gravity g is 1.31 m s^{-2} for Europa.

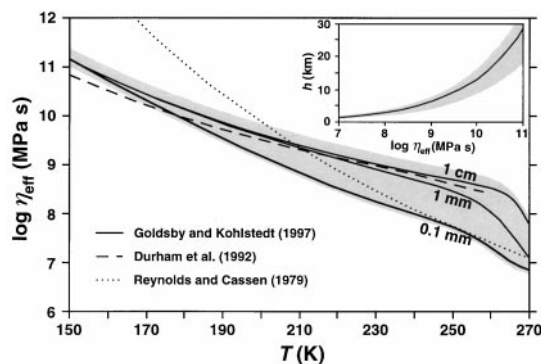


Figure 2 Effective viscosity η_{eff} of ice as a function of temperature *T*, strain rate $\dot{\epsilon}$, and grain size *d* for conditions relevant to the subsurface of Europa. Solid lines represent a grain-size-sensitive flow law for ice^{15,16} (extrapolated to lower temperatures from the experimental conditions of $173 \text{ K} \leq T \leq 248 \text{ K}$, and extended to warmer temperatures on the basis of unpublished data of D.L.G. and D. L. Kohlstedt), for a nominal Europa strain rate⁵ of $\dot{\epsilon} = 2 \times 10^{-10} \text{ s}^{-1}$, and varying with grain size as labelled. The shaded region represents η_{eff} for a likely range in European subsurface conditions, from $\dot{\epsilon} = 1 \times 10^{-10} \text{ s}^{-1}$ and $d = 1 \text{ cm}$ (upper bound of shaded region) to $\dot{\epsilon} = 3 \times 10^{-10} \text{ s}^{-1}$ and $d = 0.1 \text{ mm}$ (lower bound). At relatively warm temperatures, η_{eff} varies by an order of magnitude over the range of conditions considered. The dotted line represents the temperature-dependent relationship for ice viscosity adopted by Reynolds and Cassen¹⁴, and the dashed line represents the power-law (grain-size independent) ice flow relationship of Durham *et al.*²⁹ (derived over the temperature range $195 \text{ K} \leq T \leq 258 \text{ K}$ and extrapolated here to lower temperatures). Inset, Critical layer thickness *h* as a function of η_{eff} for the onset of convection on Europa as predicted by equation (1). Solid line indicates the nominal case of $Ra = 2,000$; upper and lower bounds of the shaded region correspond to $Ra = 3,500$ and 500, respectively.

Parameter values for ice are evaluated at the average temperature appropriate to the potentially convecting sublayer, estimated as¹⁸

$$T_b = \{(Q/4R) - [(Q/4R)^2 - QT_t/R]^{1/2}\} - T_t \quad (2)$$

where Q is the activation energy for ice creep, R is the gas constant, T_b is the sublayer's lower boundary temperature (assumed to be ~ 273 K), and T_t is the upper boundary temperature. We find that grain boundary sliding ($Q = 49 \text{ kJ mol}^{-1}$)^{15,16} dominates the deformation of ice over the range of potential average sublayer temperatures, for the grain sizes and stresses modelled for Europa (see below), giving $T_t = 197$ K and $\Delta T = 76$ K. For ice¹⁹ at $T_{\text{ave}} = 235$ K: density $\rho = 923 \text{ kg m}^{-3}$, thermal expansivity $\alpha = 1.4 \times 10^{-4} \text{ K}^{-1}$, and thermal diffusivity $\kappa = 1.4 \times 10^{-6} \text{ m}^2 \text{ s}^{-1}$.

Previous analyses of solid-state convection on icy satellites^{14,20} have assumed a strictly temperature-dependent viscosity for ice. The effective viscosity η_{eff} of a non-newtonian material such as ice is more accurately defined as

$$\eta_{\text{eff}} = \sigma / (3\dot{\epsilon}_{\text{tot}}) \quad (3)$$

where either stress σ or strain rate $\dot{\epsilon}$ is assumed fixed. Several processes may deform Europa's ice shell on a long timescale ($> 10^5$ yr) including non-synchronous rotation^{21,22}, polar wander²³, and viscous flow from thick towards thin portions of an ice shell²³. However, far more rapid straining is induced by tidal deformation as the satellite travels through its 3.6-day elliptical orbit²¹. This strain rate is modelled as $(1-3) \times 10^{-10} \text{ s}^{-1}$, varying with latitude and longitude⁵, and will control the effective viscosity of Europa's subsurface ice as a function of its grain size (Fig. 2). The grain size of Europa's relatively pristine surface plains inferred from Galileo imaging²⁴ is ~ 0.1 mm, and the range chosen here represents a possible increase with depth, as through sintering.

At $T_{\text{ave}} \approx 235$ K, the range of strain rates and grain sizes considered predicts $\eta_{\text{eff}} \sim 10^8-10^9$ MPa s, and corresponding stresses $\sim 0.1-0.4$ MPa. From equation (1), the corresponding thickness of the sublayer when convection initiates is $\sim 3-7$ km for $Ra \approx 2,000$, and $\sim 2-8$ km for the range of Ra considered (Fig. 2, inset). The onset of convection should vary across Europa, depending on local heat flow, strain rate and ice grain size. For finite-amplitude convection, the spacing of upwelling regions is predicted to be about twice the sublayer thickness, nominally $\sim 6-14$ km for Europa; although the convective state in Europa's ice shell may not be related to the linear state at the onset of convection, this dimension is remarkably similar to the $\sim 5-20$ km spacing of Europa's domes, pits and spots.

The thickness of Europa's whole ice shell when convection initiated can be estimated if the thickness of the overlying rheological lithosphere is known. The degree of thermal and mechanical alteration revealed by pits and micro-chaos regions suggests intrusion of warm diapirs to a few kilometres depth or less; moreover, a variety of geological analyses suggest that the thickness of Europa's overlying brittle lithosphere was probably ≤ 2 km thick^{1,25,26} at the time of its deformation. This suggests a total ice shell thickness of $\sim 3-10$ km. This is significantly less than the 30 km value of Reynolds and Cassen¹⁴, who derived an upper-limit shell thickness of initiation of convection, and who used a strictly temperature-dependent viscosity relationship. Our value is also less than the $\sim 10-30$ km whole-shell thickness predicted by thermal modelling⁵, which assumes the absence of convection. We estimate the vertical scale of Europa's upward domes as < 100 m, based on comparison with nearby features that cast shadows; a rise of warm ice through a $\sim 3-10$ km ice shell to a level of neutral buoyancy is consistent with this inferred topography, though the precise buoyancy forces would be affected locally by the presence of salts, the topography of the warm and cold ice layers, and the rise and cooling rates of diapirs.

Overall, we find strong similarity between the morphology, geometry and spacing of surface features plausibly interpreted as due to diapirism, and revised predictions for the onset of convection

in a floating ice shell on Europa. If a european shell cooled and thickened above a liquid water interior to the point where solid-state convection initiated regionally, the geological style may have changed from widespread tectonism associated with a thin ice shell to vertical deformation linked to diapirism. This is consistent with the stratigraphic history observed until now, in that pits, domes and spots consistently disrupt linear features but are rarely cut by them. Examples of domes, pits and spots surrounding, and apparently within, a large area of chaos¹ imaged by Galileo suggest that this chaos area may represent a region of intense diapiric upwelling, perhaps related to local variations in heat flux, instability development, or thickness of the rigid surface layer, and so does not provide certain evidence of melting.

Solid-state convection is an efficient heat loss mechanism, predicted to freeze a european ocean² in $\sim 10^8$ yr, unless sufficient heat is continually supplied to the convecting ice, for example through tidal heating. Indeed, because tidal dissipation is greatest in the warmest portion of an ice shell⁵, tidal dissipation may be enhanced in a floating ice shell warmed throughout by convection, perhaps allowing an ocean to be maintained²⁷.

Although gravity measurements suggest that Europa is differentiated, with an outer H₂O layer ~ 150 km thick²⁸, its state (completely solid, or a solid shell above liquid) is not directly addressed by the gravity data. Models for Europa diapirism could be proposed that do not require a liquid layer, for example solid-state convection of a thick ice layer with convection driven by a steep thermal gradient, or diapiric instability driven by compositional layering; however, explicit modelling of such schemes is necessary to evaluate their consistency with the observations and interpretations we have described. We have shown that the geological observations and implications of pits, domes and spots are consistent with a model of diapirism as representative of convection in a floating ice shell. In combination with the low crater density and inferred young surface age of Europa¹, this increases the likelihood that liquid water may persist to the present day beneath the surface of Europa. Continuing Galileo imaging and morphological analyses, along with additional modelling of Europa's internal configuration and heat balance, will further test this idea. \square

Received 28 May; accepted 3 November 1997.

- Carr, M. H. *et al.* Evidence for a subsurface ocean on Europa. *Nature* **391**, 363-365 (1998).
- Cassen, P. M., Peale, S. J. & Reynolds, R. T. in *Satellites of Jupiter* (ed. Morrison, D.) 93-128 (Univ. Arizona Press, Tucson, 1982).
- Squyres, S. W., Reynolds, R. T., Cassen, P. & Peale, S. J. Liquid water and active resurfacing on Europa. *Nature* **301**, 225-226 (1983).
- Ross, M. & Schubert, G. Tidal heating in an internal ocean model of Europa. *Nature* **325**, 133-134 (1987).
- Ojakangas, G. W. & Stevenson, D. J. Thermal state of an ice shell on Europa. *Icarus* **81**, 220-241 (1989).
- Lucchitta, B. K. & Soderblom, L. A. in *Satellites of Jupiter* (ed. Morrison, D.) 521-555 (Univ. Arizona Press, Tucson, 1982).
- Carr, M. H. *et al.* The Galileo Imaging Team plan for observing the satellites of Jupiter. *J. Geophys. Res.* **100**, 18935-18955 (1995).
- Greeley, R. *et al.* Europa triple bands: Galileo images. *Lunar Planet. Sci. Conf. Abstr.* **28**, 455-456 (1997).
- Kargel, J. S. Brine volcanism and the interior structures of asteroids and icy satellites. *Icarus* **94**, 368-390 (1991).
- Jenyon, M. K. *Salt Tectonics* (Elsevier, New York, 1986).
- O'Brien, G. D. *Mem. Am. Assoc. Petrol. Geol.* **8**, 1-9 (1968).
- Schenk, P. & Jackson, M. P. A. Diapirism on Triton: A record of crustal layering and instability. *Geology* **21**, 299-302 (1993).
- Schubert, G., Spohn, T. & Reynolds, R. T. in *Satellites* (eds Burns, J. A. & Matthews, M. S.) 224-292 (Univ. Arizona Press, Tucson, 1986).
- Reynolds, R. T. & Cassen, P. M. On the internal structure of the major satellites of the outer planets. *Geophys. Res. Lett.* **6**, 121-124 (1979).
- Goldsbey, D. L. & Kohlstedt, D. L. Flow of ice I by dislocation, grain boundary sliding, and diffusion processes. *Lunar Planet. Sci. Conf. Abstr.* **28**, 429-430 (1997).
- Goldsbey, D. L. & Kohlstedt, D. L. Grain boundary sliding in fine-grained ice I. *Scripta Mat.* **37**, 1399-1406 (1997).
- Stengel, K. C., Oliver, D. S. & Booker, J. R. Onset of convection in a variable viscosity fluid. *J. Fluid Mech.* **120**, 411-431 (1982).
- Mueller, S. & McKinnon, W. B. Three-layered models of Ganymede and Callisto: Compositions, structures, and aspects of evolution. *Icarus* **76**, 437-464 (1988).
- Hobbs, P. V. *Ice Physics* (Clarendon, Oxford, 1974).
- Squyres, S. W. & Croft, S. K. in *Satellites* (eds Burns, J. A. & Matthews, M. S.) 293-341 (Univ. Arizona Press, Tucson, 1986).
- Greenberg, R., Geissler, P., Pappalardo, R. & Galileo Imaging Team. Long term and 'diurnal' tidal stresses on Europa. *Lunar Planet. Sci. Conf. Abstr.* **28**, 457-458 (1997).

22. Geissler, P. E. *et al.* Evidence for non-synchronous rotation of Europa *Nature* **391**, 368–370 (1998).
 23. Ojakangas, G. W. & Stevenson, D. J. Polar wander of an ice shell on Europa. *Icarus* **81**, 242–270 (1989).
 24. Geissler, P. E., Phillips, C. & Denk, T. in *Proc. Workshop on Remote Sensing of Planetary Ices: Earth and Other Solid Bodies* 8.5 (1997).
 25. Pappalardo, R. *et al.* Deformation and properties of Europa's lithosphere. *Eos* **78**, S203 (1996).
 26. Williams, K. K. *et al.* Estimates of ice thickness on Europa. *Eos* **78**, F415–F416 (1997).
 27. McKinnon, W. B. Convective instabilities in Europa's floating ice shell. *Bull. Am. Astron. Soc.* **29**, 984 (1997).
 28. Anderson, J. D. *et al.* Europa's differentiated internal structure: Inferences from two Galileo encounters. *Science* **276**, 1236–1239 (1997).
 29. Durham, W. B., Kirby, S. H. & Stern, L. A. Effects of dispersed particulates on the rheology of water ice at planetary conditions. *J. Geophys. Res.* **97**, 20883–20897 (1992).

Acknowledgements. We thank W. McKinnon and N. Sleep for reviews; N. Sherman, L. Prockter and G. Collins for their contributions; and J. Kaufman, K. Magee and K. Klaasen for their efforts in acquisition of the E6 Europa imaging data. This work was supported by NASA's Galileo Project.

Correspondence and requests for materials should be addressed to R.T.P. (e-mail: robert_pappalardo@brown.edu).

Evidence for non-synchronous rotation of Europa

P. E. Geissler*, R. Greenberg*, G. Hoppa*, P. Helfenstein†, A. McEwen*, R. Pappalardo‡, R. Tufts*, M. Ockert-Bell†, R. Sullivan||, R. Greeley||, M. J. S. Belton§, T. Denk¶, B. Clark†, J. Burns†, J. Veverka† & the Galileo Imaging Team

* Lunar and Planetary Laboratory, University of Arizona, Tucson, Arizona 85712, USA

† Laboratory for Planetary Science, Cornell University, Ithaca, New York 14853, USA

‡ Department of Geological Sciences, Box 1846, Brown University, Providence, Rhode Island 02912, USA

§ National Optical Astronomy Observatories, PO Box 26732, Tucson, Arizona 85726, USA

|| Department of Geology, Arizona State University, Box 871404, Tempe, Arizona 85287, USA

¶ DLR, Institute for Planetary Exploration, Rudower Chaussee 5, 12489 Berlin, Germany

Non-synchronous rotation of Europa was predicted on theoretical grounds¹, by considering the orbitally averaged torque exerted by Jupiter on the satellite's tidal bulges. If Europa's orbit were circular, or the satellite were comprised of a frictionless fluid without tidal dissipation, this torque would average to zero. However, Europa has a small forced eccentricity $e \approx 0.01$ (ref. 2), generated by its dynamical interaction with Io and Ganymede, which should cause the equilibrium spin rate of the satellite to be slightly faster than synchronous. Recent gravity data³ suggest that there may be a permanent asymmetry in Europa's interior mass distribution which is large enough to offset the tidal torque; hence, if non-synchronous rotation is observed, the surface is probably decoupled from the interior by a subsurface layer of liquid⁴ or ductile ice¹. Non-synchronous rotation was invoked to explain Europa's global system of lineaments and an equatorial region of rifting seen in Voyager images^{5,6}. Here we report an analysis of the orientation and distribution of these surface features, based on initial observations made by the Galileo spacecraft. We find evidence that Europa spins faster than the synchronous rate (or did so in the past), consistent with the possibility of a global subsurface ocean.

Several testable predictions can be based on the hypothesis of non-synchronous rotation of Europa. First, systematic changes in the orientation of lineaments with age may be expected as the surface reorients relative to fixed global patterns of tidal stress. Second, crustal extension is predicted in the regions west of the tidal bulges as the surface stretches to accommodate the changing shape. Third, no asymmetry in impact crater density between leading and trailing hemispheres should be found if Europa's surface has rotated continually with respect to Jupiter. Last, if the rotation rate is large

enough, the locations of surface features seen in Galileo images might be displaced eastwards relative to their positions in Voyager data. Galileo Solid State Imaging (SSI) data represent a substantial improvement over Voyager data in terms of spatial resolution, spatial coverage and spectral range of the observations. After four close passes of Europa and several non-targeted encounters⁷, samples of the surface at various locations have been imaged at resolutions down to 20 m per pixel; coverage has been expanded especially on the trailing hemisphere, and observations of Europa's surface at near-infrared wavelengths have revealed lineaments invisible to Voyager bandpass filters.

Galileo colour data provide one test of non-synchronous rotation. Multispectral imaging of Europa's northern high-latitude region was performed during Galileo's first orbit of Jupiter⁷. The imaged region extends across the trailing side of the anti-jovian hemisphere, centred at 45° N, 221° W. False-colour composites made up from these images show at least three distinct classes of linear features on Europa's surface (Fig. 1). These features may represent different stages of development of tectonic lineaments on Europa. Their distributions are shown in Fig. 2, derived from photogeological and spectral mapping (supervised classification) of the photometrically corrected four-colour data. Bands with spectral reflectance similar to the bright wedge (Fig. 2a) make up the stratigraphically oldest lineaments and generally have southwest–northeast trends. The intermediate-aged triple-bands (Fig. 2b) trend roughly east–west, with the younger of the two

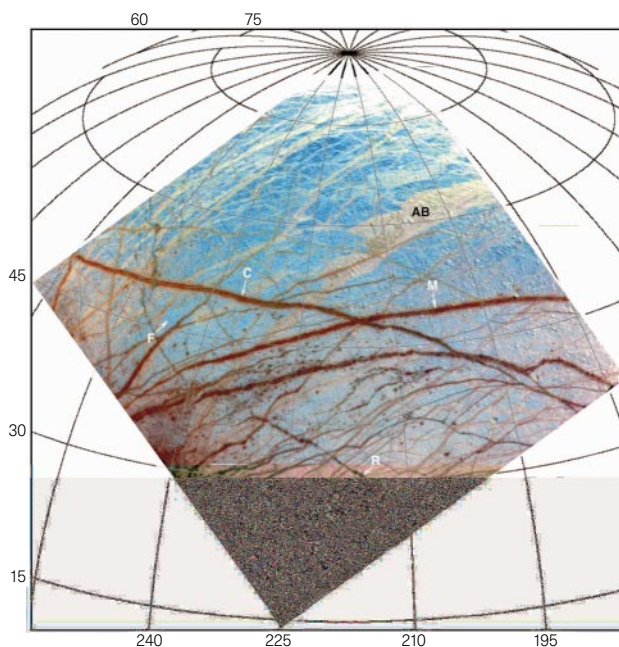


Figure 1 False-colour composite of northern high-latitude region of Europa, produced from images taken through the 968-nm, 756-nm and green filters. Overlaid is a grid showing location in degrees North latitude and West longitude. The most prominent linear features are the dark triple-bands such as Cadmus Linea and Minos Linea. The triple-bands overprint many older lineaments which are intermediate in colour between the triple-bands and the icy plains, but are brighter than the triple-bands and the surrounding icy plains at near-infrared wavelengths. These older lineaments include a bright wedge at 60° N, 200° W, which is somewhat similar to the grey bands identified in the southern polar regions in Voyager images¹⁴. The youngest features appear to be incipient fractures, less than a pixel (1.6 km) wide, which cross-cut the dark triple bands. Labelled on this figure, in order of age (as determined from cross-cutting relationships), are young fractures (F), developing band Rhadamanthys Linea (R), intermediate-aged triple bands Cadmus Linea (C) and Minos Linea (M), and a wedge-shaped ancient band (AB).